Physica C: Superconductivity and its applications 621 (2024) 1354515

Contents lists available at ScienceDirect

Physica C: Superconductivity and its applications

journal homepage: www.elsevier.com/locate/physc

Full Length Article

Investigation of superconductivity of A15 type cubic Nb_3Os material by using density functional theory

Fatih Kurtuluş [a,b,*], Ertuğrul Karaca [c,d,e], Sadık Bağcı [b]

[a] Sakarya University of Applied Science, Arifiye Vocational High School, 54330 Sakarya, Turkey
[b] Department of Physics, Sakarya University, Esentepe Campus, 54187, Sakarya, Turkey
[c] Sakarya University, Biomedical, Magnetic, and Semiconductor Materials Research Center (BIMAS-RC), 54187 Sakarya, Türkiye
[d] Centre for Advanced Laser Techniques, Institute of Physics, 10000 Zagreb, Croatia
[e] Department of Physics, University of York, York, YO10 5DD, UK

ARTICLE INFO

Keywords:
Superconductivity
Density functional theory
Electronic properties
Phonons

ABSTRACT

In this study, the structural, elastic, electronic, phonon and electron-phonon interaction properties of A15 type cubic Nb_3Os compound were investigated by density functional theory. The lattice constant of this compound was obtained in agreement with experiments, and the investigation of elastic properties revealed its ductile nature. From electronic calculations for Nb_3Os, the density of states at Fermi level ($N(E_F)$) was found to be 5.31 states/eV with the largest contribution of Nb 4d orbitals. According to the results obtained from phonon calculations, Nb_3Os was found to be dynamically stable in the cubic A15 structure and phonon modes were largely formed by the vibrations of Nb atoms. Using the electronic and phonon properties, we determined the Eliashberg spectral function, which illustrates the electron-phonon interaction. The electron-phonon interaction parameter and average phonon frequency values for Nb_3Os were found to be 0.41 and 222.97 K, respectively. The calculated superconducting transition temperature of 1.05 K is in excellent agreement with the experimental value of 1.02 K.

1. Introduction

The A15 phase (also known as the β-W or Cr_3Si structure type), usually with the chemical formula A_3B, is the equilibrium phase for intermetallic compounds, where A represents a transition element, while B can be both a transition and non-transition element. Most of these compounds show superconductivity at relatively high temperatures around 20 K and high magnetic fields on the order of a few tens of tesla [1]. Until compounds with high superconducting temperatures were found in 1986 [2], the A15 type material with the highest superconducting transition temperature (T_c) is Nb3Ge with 23.2 K [3]. Due to this high Tc value of Nb_3Ge compound, Nb-based Nb_3X compounds with the same structure have been intensively studied until today. One of these compounds, Nb_3Os, is available in the literature.

The superconducting transition temperature of Nb_3Os compound was experimentally determined as 1.02 K in 1963 and 0.943 K in 1969 [4,5]. After it was determined that Nb3Os is a superconductor, different experimental studies were carried out on the structural and superconducting properties of this compound [6-8]. In addition to these experimental studies, there are two theoretical articles in 1999 and 2007 in which the structural and electronic properties of Nb3Os were examined with the full-potential-linearized-augmented-plane-waves FLAPW method [9,10]. In another theoretical study conducted with density functional theory (DFT), the structural, elastic and electronic properties of Nb3Os were examined [11]. According to our literature search, the structural, electronic and elastic properties of Nb_3Os compound have been theoretically investigated in detail, but no theoretical study examining its phonon and superconducting properties has been found. In this study, our aim is not to obtain a new superconductor but to theoretically determine the source of superconductivity of Nb_3Os compound.

The most effective way to determine the electron-phonon interaction, which is necessary to understand the origin of superconductivity, is to determine the Eliashberg spectral function ($\alpha^2F(\omega)$), which includes electrons, phonons and the contribution from this interaction [12-18]. So far, this function has not been investigated for Nb_3Os material. In this study, the structural, electronic, elastic, phonon and superconductivity properties of Nb_3Os compound were investigated in detail using density

* Corresponding author.
E-mail address: fatihkurtulus@subu.edu.tr (F. Kurtuluş).

https://doi.org/10.1016/j.physc.2024.1354515
Received 24 February 2024; Received in revised form 6 April 2024; Accepted 29 April 2024
Available online 4 May 2024

functional theory. In this context, the electronic density of states at the Fermi level ($N(E_F)$), the Eliashberg spectral function ($\alpha^2F(\omega)$) and the electron-phonon interaction parameter (λ) were determined. Based on these data, the superconducting transition temperature (Tc) of Nb_3Os material was calculated. The superconductivity results are compared with existing experimental and theoretical findings.

2. Calculation method

Quantum mechanical calculations were performed using the QUANTUM ESPRESSO Ab initio simulation package [19] based on plane wave and pseudopotential methods and density functional theory. Pseudopotentials obtained by Perdew-Burke-Ernzerhof [20] using the generalised gradient approximation (GGA) were used to model electron-ion interactions. The Kohn-Sham [21] equations were solved using the Monkhorst-Pack [22] special $\vec{k}$ points, a set within the Brillouin zone. A network of $8 \times 8 \times 8$ $\vec{k}$ points was used to calculate the total energy values of the Nb_3Os compound. For electronic structure and electronic density of states calculations, a $32 \times 32 \times 32$ $\vec{k}$-point mesh was used. The phonon frequencies were calculated using the linear-response method [19] as implemented in the Quantum-Espresso ab initio simulation package [19]. For phonon calculations, 10 dynamical matrices corresponding to a $4 \times 4 \times 4$ $\vec{q}$-point mesh were used. In addition, by using the Migdal-Eliashberg theory [23,24], the Eliashberg spectral function is expressed the equation below.

$$\alpha^2F(\omega) = \frac{1}{2\pi N(E_F)} \sum_{\vec{q}j} \frac{\gamma_{\vec{q}j}}{\hbar\omega_{\vec{q}j}} \delta(\omega - \omega_{\vec{q}j}) \tag{1}$$

Here $N(E_F)$ is density of states at Fermi level, $\gamma_{\vec{q}j}$ is the phonon linewidth and $\omega_{\vec{q}j}$ is the phonon frequencies. The average electron-phonon interaction parameter is

$$\lambda = 2 \int \frac{\alpha^2F(\omega)}{\omega} d\omega. \tag{2}$$

After the electron-phonon interaction parameter is calculated, the logarithmic average phonon frequency ω_{ln}, expressed by the following equation.

$$\omega_{ln} = exp\left[2\lambda^{-1} \int_0^\infty \frac{d\omega}{\omega} \alpha^2F(\omega) ln\omega\right] \tag{3}$$

Finally, the superconducting transition temperature is obtained from the equation below.

$$T_c = \frac{\omega_{ln}}{1.2} exp\left(\frac{-1.04(1+\lambda)}{\lambda - \mu(1+0.62\lambda)}\right) \tag{4}$$

In this equation, μ^* denotes the screened repulsive Coulomb potential having values between 0.10 and 0.16 [25,26]. In this ab initio calculation for Nb_3Os its value is chosen as 0.10.

3. Results and discussion

3.1. Structural properties of Nb_3Os compound

The Nb_3Os compound has a cubic A15 structure and its crystal structure belongs to the space group $Pm\bar{3}n$ (No:223) with the Pearson symbol cP8. There are 6 Nb atoms and 2 Os atoms in a unit cell. The Wyckoff positions of Nb and Os atoms are as follows; (6c) (1/4, 0, 1/2) for 6 Nb atoms and (2a) (0,0,0) for 2 Os atoms. The A15 type cubic crystal structure of the Nb_3Os compound obtained as a result of the calculations is shown in Fig. 1a. The high symmetry points on the first Brillouin zone of the simple cubic lattice are presented in Fig. 1b. In this figure, the high symmetry points are Γ(0,0,0), X(0.0,0.5,0.0), M (0.5,0.5,0.0) and R(0.5,0.5,0.5). The calculated bond length value between Nb and Os atoms was found to be 2.891 Å, which is slightly shorter than the sum of the covalent radii of niobium and osmium atoms, which are 1.64 Å and 1.44 Å, respectively [27,28]. This result indicates that these atoms are bound by a mixture of ionic and covalent interactions. The calculated bond length value between Nb and Nb atoms was found to be 2.585 Å, which is significantly shorter than that of volume-centred cubic niobium, where each niobium atom has eight neighbours at 2.86 Å [29]. These results indicate strong bond strengths between the Nb atoms in the studied compound. In addition, the calculated bond lengths are consistent with the values previously obtained by Naher and co-workers [11]. At the beginning of our calculations, the total energy corresponding to certain lattice constants around the equilibrium value was calculated and the graph of the energy dependent on the lattice constant shown in Fig. 2 was drawn using the calculated total energy values and the Murnaghan equations [30] given below. The equilibrium lattice constant (a), volume modulus (B_0) and the first derivative of the volume modulus with respect to pressure (B_0') corresponding to the point where the compound is most stable were obtained from this fit.

$$P = \frac{B_0}{B_0'} \left[\left(\frac{\Omega_0}{\Omega}\right)^{B_0'} - 1\right] \tag{5}$$

$$E = \frac{\Omega_0 B_0}{B_0'} \left[\frac{1}{B_0' - 1}\left(\frac{\Omega}{\Omega_0'}\right)^{B_0'-1} + \frac{\Omega}{\Omega_0}\right] - \frac{\Omega_0 B_0}{B_0' - 1} + E(\Omega_0) \tag{6}$$

Here, Ω is the volume and B_0 is the bulk modulus. The calculation of the bulk modulus, which is a measure of the durability of crystals in terms of their efficient use in technological applications, is extremely important The obtained equilibrium parameters (a, B_0 and B_0') and bond lengths ($d_{Nb\text{-}Nb}$, $d_{Nb\text{-}Os}$) are presented in Table 1. The lattice parameter $a = 5.17$ Å, the bulk modulus $B = 218.7$ GPa and the first derivative of the bulk

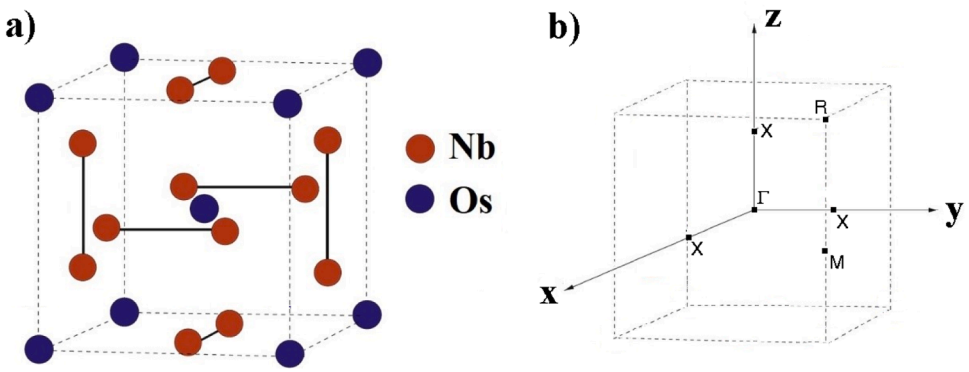

Fig. 1. a) Representation of the crystal structure for the compound Nb_3Os. b) The high symmetry points on the first Brillouin zone of the simple cubic lattice.

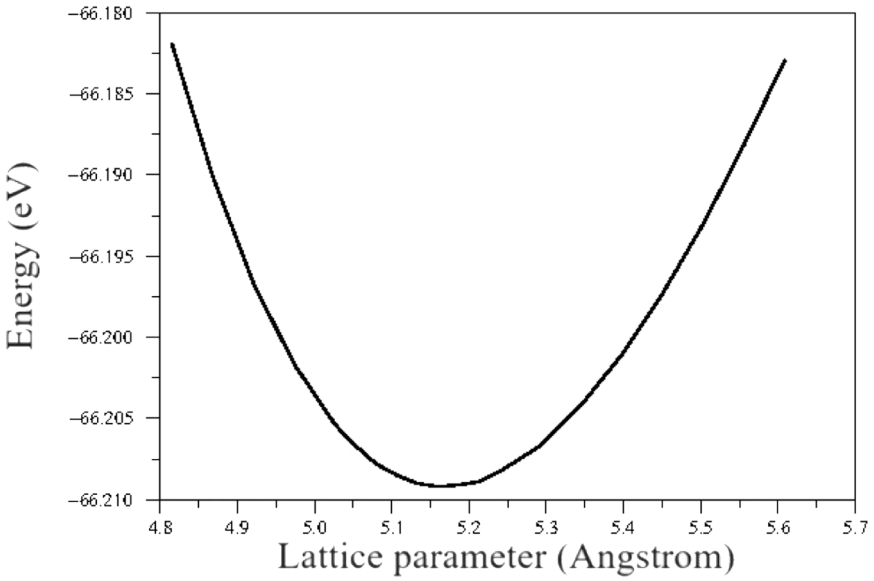

Fig. 2. Plot of energy versus lattice constant for Nb_3Os compound.

Table 1
The structural parameters calculated for the cubic Nb_3Os compound are presented in the table. Additionally, the results obtained were compared with experimental and theoretical values in the literature.

	a (Å)	$d_{Nb\text{-}Nb}$ (Å)	$d_{Nb\text{-}Os}$ (Å)	B(GPa)	B′
This work	5.17	2.585	2.891	218.7	3.91
Experimental [31,32]	5.14				
GGA [11]	5.16	2.580	2.900	225.26	
GGA [10]	5.18			218.78	

modulus with respect to pressure B' = 3.91 were calculated. These values are in agreement with previous experimental [31,32] and theoretical results [10,11].

3.2. Electronic properties of Nb_3Os compound

The electronic energy band structure graph calculated using structural parameters for Nb_3Os compound is shown in Fig. 3. When the band structure is examined, several bands cut the Fermi level. This indicates that the compound under investigation has a metallic structure. Additionally, the graph shows that there is an almost flat band in a short region at the end of the Γ-X direction corresponding to the Fermi level. This flat band has the potential to form a strong peak close to the Fermi level. This is an important feature for superconductivity because BCS theory clearly states that the electrons forming Cooper pairs are those with energies close to the Fermi level. The obtained electronic band structure graph is in good agreement with previous theoretical studies [10,11]. This agreement is a sign that the results obtained for the electronic structure are reliable.

The total and partial energy density of state graphs obtained for the Nb_3Os compound are given in Fig. 4. The vertical dashed line indicates the Fermi level. As seen in Fig. 4, the largest contribution to the formation of valence bands in the region between approximately −7.2 eV and −5.0 eV comes from Nb 5p electrons. From −5.0 eV to the Fermi energy level, it is clearly seen that Nb 4d electrons make the largest

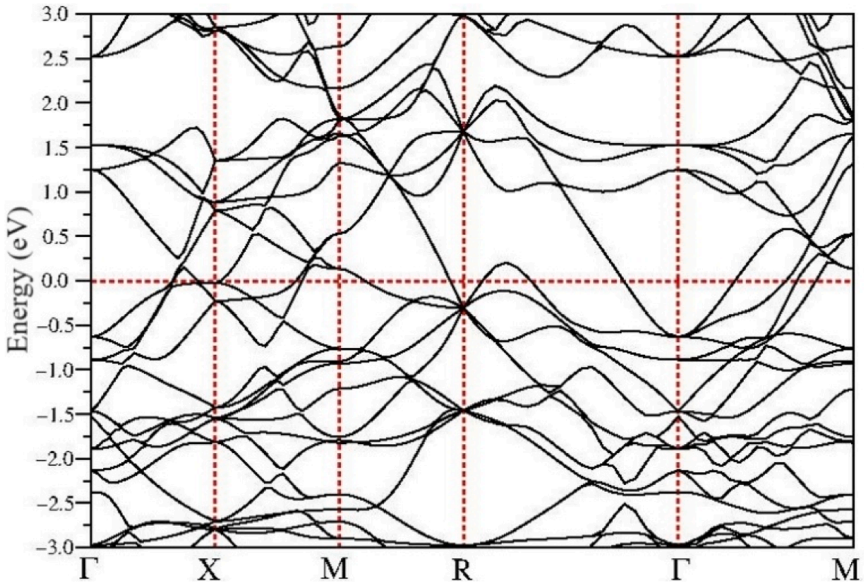

Fig. 3. The electronic band structure graph calculated for the Nb_3Os compound is presented. In the graph, the Fermi energy level is taken as 0 eV.

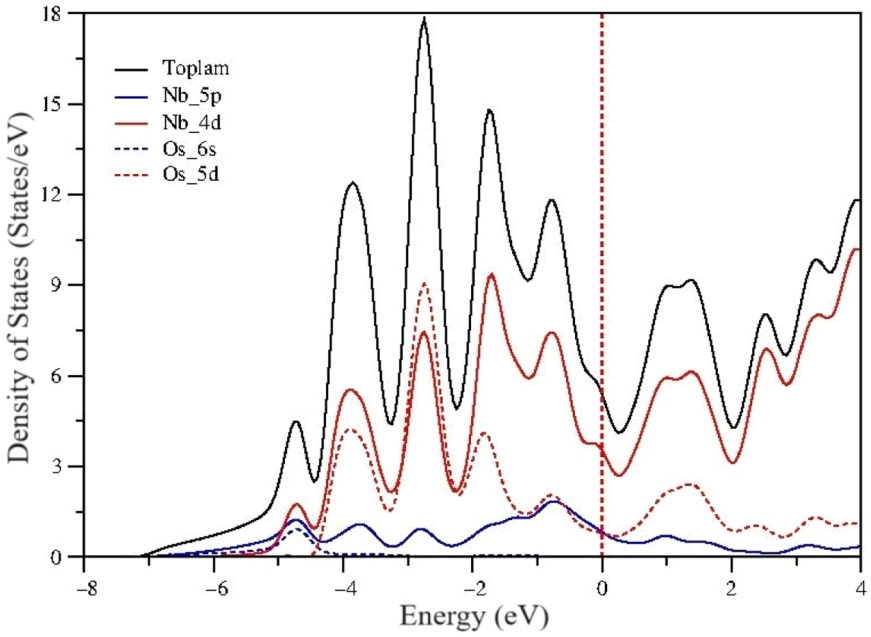

Fig. 4. Density of electronic states for the compound Nb_3Os.

contribution to the formation of energy bands. However, in the region between −3.0 eV and −2.0 eV, Os 5d electrons are found to be more dominant. The formation of conduction bands above the Fermi level is largely caused by Nb 4d electrons as seen in Fig. 4. As mentioned before, Fermi energy level density of states ($N(E_F)$) is an important parameter according to BCS theory in the investigation of superconductivity properties of a material. The $N(E_F)$ value obtained for Nb_3Os was found to be 5.31 states/eV. As seen, the largest contribution to the formation of this density of states comes from Nb 4d electrons. The state density values obtained for the Fermi energy level are in agreement with previous theoretical results [10,11].

3.3. Elastic properties of Nb_3Os compound

Electron-phonon interaction plays an important role in defining the superconductivity properties of a material. As it is known, the phonon properties obtained for a material are in a relationship with its elastic properties. Therefore, it can be expected that the superconducting properties and elastic properties obtained by electron-phonon interaction are also related to each other. Considering this relationship, the study of the elastic properties of superconducting compounds has an important place in the theoretical understanding of the superconducting properties of the compound. In addition, the mechanical stability and hardness of the compounds can be obtained by using elastic constants and these results provide useful data in determining their application areas. There are three independent constants in the simple cubic lattice, namely C_{11}, C_{12} and C_{44}. In this study, their calculation was carried out using the well-known strain-stress method presented by the thermopw code [33]. The elastic constants calculated for Nb3Os by this method and the results obtained from previous theoretical studies [11] are presented in Table 2. When the table is examined, it is seen that all elastic constant results are consistent with the previous data. In cubic structures, C_{11}, C_{12} and C_{44} are non-zero elastic constants. In order to determine that a crystal is stable in a cubic structure, Born criteria [34,35] must be met. These criteria are;

$$C_{11} > 0;\ C_{44} > 0;\ C_{11} - C_{12} > 0;\ C_{11} + 2\,C_{12} > 0 \tag{7}$$

is in the form. When the values in Table 2 are examined, it is seen that these conditions are met for Nb_3Os compound. This result shows that Nb_3Os compound is mechanically stable in A15 type cubic crystal structure.

The Voigt-Reuss-Hill (VRH) method [36] can be used to calculate the bulk modulus (B) and shear modulus (G) values using the elastic constants C_{11}, C_{12} and C_{44} obtained for the Nb_3Os compound. The volume modulus expression is defined in the same way by Voigt and Reuss,

$$B_V = B_R = \frac{1}{3}(C_{11} + 2C_{12}) \tag{8}$$

can be calculated using the formula. The shear modulus can be calculated using elastic constants with different formulas given by Voigt and Reuss as follows [37-39].

$$G_V = \frac{1}{5}(C_{11} - C_{12} + 3C_{44}) \tag{9}$$

$$G_R = \frac{5.(C_{11} - C_{12})C_{44}}{4C_{44} + 3(C_{11} - C_{12})} \tag{10}$$

The averages of the bulk modulus and shear modulus values are;

$$B_H = (B_V + B_R)/2 \tag{11}$$

$$G_H = (G_V + G_R)/2 \tag{12}$$

is given as. After calculating the bulk modulus and shear modulus, Young's modulus (E) and Poisson's ratio (ν) can be obtained by using these results and utilising the following equations [40].

$$E = \frac{9BG}{3B + G} \tag{13}$$

Table 2
Individual elastic constants (C_{11}, C_{12} and C_{44}) (in GPa), isotropic bulk modulus B_H (in GPa), shear modulus G_H (in GPa), young modulus E_H (in GPa), B_H/G_H ratio and Poisson's ratio (ν) were calculated for the cubic Nb_3Os compound and compared with previous theoretical and experimental data.

	C_{11}	C_{12}	C_{44}	B_H	G_H	E_H	B_H/G_H	ν
This work	399.2	135.7	63	223.5	85.1	226.5	2.63	0.33
GGA [11]	413.1	131.3	67.3	225.3	90.9	240.3	2.48	0.32

$$\nu = \frac{3B - 2G}{2(3B + G)} \tag{14}$$

The bulk modulus (B_H), shear modulus (G_H) and young's modulus (E_H), Poisson's ratio (ν) and B_H/G_H ratio values calculated for Nb_3Os compound using VRH method are given in Table 2. When Table 2 is analysed, it is seen that the calculated values are in satisfactory agreement with the theoretical values. Poisson's ratio ($-1 \leq \nu \leq 0.5$) is used to measure the stability of crystals against shear deformation [41]. The elasticity and brittleness of materials can be understood by comparing Poisson's ratios, Cauchy pressure and B_H/G_H ratios. Materials with an improved ductility should have a larger Poisson's ratio and B_H/G_H ratio. Poisson's ratio $\nu > 0.26$, Cauchy pressure C_{12} - $C_{44} > 0$ and $B_H/G_H > 1.75$ distinguish ductile material from brittle material. When Table 2 is examined, it is seen that Nb_3Os compound meets the ductility conditions.

3.4. Vibrational properties of Nb_3Os compound

The phonon dispersion graph obtained for the Nb_3Os compound as a result of the calculations is shown in Fig. 5a. It is well known that the 8 atoms in the unit cell of the Nb3Os compound generate 24 phonon modes. Three of these modes are acoustic and the other 21 are optical modes. While 2 of the 3 acoustic modes are transverse acoustic (TA) and 1 is longitudinal acoustic (LA), similarly, 14 of the 21 optical modes are transverse optic (TO) and 7 are longitudinal optic (LO) modes. However, some modes overlap due to the symmetry of simple cubic lattice, and therefore these 24 modes are not visible for all directions and symmetry points in Fig. 5a. There are eight optical phonon modes at Γ point. Six of them are 3-fold degenerate, one phonon mode is 2-fold degenerate and other one is not degenerate. Similarly, there are 12 double degenerate phonon modes at X point. At point M, there are 6 double degenerate modes and the others are not degenerate. Finally, at point R, there are a total of 5 phonon modes, three of which are 6-fold degenerate, one is 4-fold degenerate, and the other is 2-fold degenerate. It is well known that the elementary excitations of a solid are described by eigenvectors and eigenfrequencies reflecting the strength of interatomic interactions. Owing to the symmetry (space group) of the equilibrium structure there are constraints for the individual eigenvectors. In special high-symmetry cases, phonon eigenvectors can even be predicted merely on the basis of group-theoretical considerations. Due to these symmetry restrictions, phonon modes may become degenerate at high symmetry points.

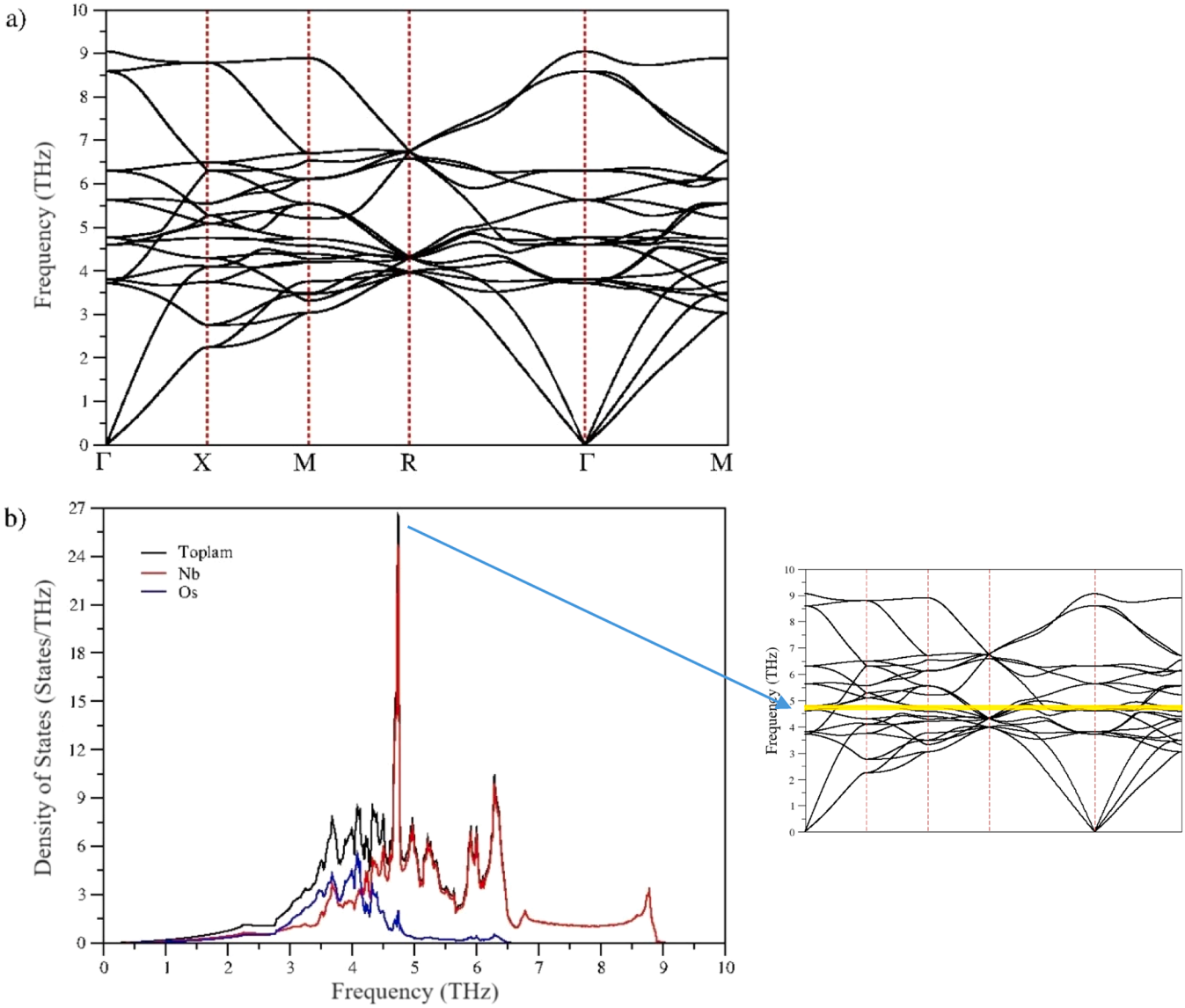

Fig. 5. a) Phonon dispersion graph calculated for Nb_3Os compound b) Phonon density of states graph obtained for Nb_3Os compound. Additionally, the phonon dispersion graph is presented, where the phonon modes that produce the highest intensity peak are highlighted.

The zone centre phonon modes at the Γ point for the Nb_3Os compound are described by the following equation.

$$\Gamma(O_h) = T_{1g} + T_{2g} + 2T_{1u} + 2T_{2u} + E_g + A_{2g} \quad (15)$$

Here, A, E and T modes are single, double and triple degenerate. While T_{2g} and E_g Raman modes are active, T_{1u} modes are infrared active and the other modes are defined as silent. These modes are presented in Table 3. Since the vibrational properties of Nb_3Os compound were studied for the first time in this article, there is no data to compare our results. In this table, the contributions of these phonon modes to the electron phonon interaction parameter (λ), which is an important parameter in determining superconductivity properties, are also presented. As can be seen from the table, the T_{1g} mode makes the largest contribution to λ.

Also, it is seen from Fig. 5a that there is no gap region between acoustic and optical modes. This is because the masses of the atoms in the unit cell are close to each other. When the phonon dispersion graph is carefully analysed, it is seen that there is no negative phonon frequency. This result is an indication that Nb_3Os compound is dynamically stable in A15 type crystal structure. The contributions of atomic vibrations to the phonon density of states can be more clearly understood by analysing the total and partial DOS plots given in Fig. 5b. In general, the partial DOS of the Nb atoms have a wide distribution over the entire range of phonon frequencies, leaving no gaps in the total phonon DOS of Nb_3Os. In particular, the partial DOS exhibits the dominance of Nb atoms in the region above 4.2 THz. This result implies that the largest contribution to the formation of optical phonon modes of Nb_3Os is due to the vibrations of Nb atoms. In the frequency range from 2.6 THz to 4.2 THz, the contribution of Os atoms to the phonon density of states is stronger. Another striking point in the phonon DOS graph is the highest intensity peak at 4.73 THz. It is well known that flat phonon dispersion bands may lead to sharp peaks in the phonon density states of compounds. In order to better see these flat phonon bands in Nb_3Os, the phonon dispersion figure, in which the phonon modes producing the highest intensity peak are highlighted, is presented in Fig. 5b. As we mentioned in the paper, there are 8 atoms in the unit cell of the Nb_3Os compound, 6 Nb and 2 Os. The fact that there are 6 Nb atoms in the unit cell, and that they bond with each other, explains their contribution to the highest intensity peak at 4.73 THz. So, for this peak, the contribution of 6 Nb atoms is much greater than the contribution of 2 Os atoms. In addition, when the eigenvectors of phonon modes with energy values that will contribute to the formation of this peak were examined for all directions in the phonon dispersion graph, it was seen that Nb atoms always vibrated much more than Os atoms at these energy values. In fact, for some energy values, Os atoms do not vibrate at all or vibrate negligibly little. For these reasons, Nb atoms play a very dominant role in the formation of the highest intensity peak at 4.73 THz.

3.5. Superconductivity properties of Nb_3Os compound

The variation of Eliashberg spectral function $\alpha^2(\omega)$ and average electron-phonon interaction parameter λ with frequency for Nb_3Os compound is given in Fig. 6. When the figure is analysed, it is determined that $\alpha^2(\omega)$ shows a great similarity with the phonon density of states. In particular, it is clearly seen in the phonon density of states graph that the highest peak value around 4.6 THz is due to the vibrations of Nb atoms. In addition, from the electronic density of states graph in Fig. 4, it is found that the largest contribution to the $N(E_F)$ value comes from Nb d electrons. When these data are taken together, it can be said that the vibrations of Nb atoms and the interactions of Nb d electrons form the basis of the superconductivity of Nb_3Os compound. The variation of λ value with frequency is also presented in Fig. 6 and λ value is calculated as 0.41. In the frequency region below 6.72 THz, λ increases with increasing frequency. Therefore, low-frequency optical phonon modes and acoustic phonon modes in this region contribute about 90.24 % to λ for Nb_3Os. The contribution of phonon modes with frequencies above 6.72 THz to λ is found to be 9.76 %. According to the BCS theory, λ plays an important role in determining the superconductivity transition temperature (T_c). Generally, T_c values of materials with high λ values are calculated higher. From this result, it can be said that the greatest contribution to the superconductivity of the Nb_3Os compound comes from the phonon modes below the frequency value of 6.72 THz. For a more detailed examination, if the phonon density of state graph in Fig. 5b and the λ graph in Fig. 6 are considered together, it is seen that the vibrations of Os atoms contribute significantly to λ, especially up to 4.2 THz. From this frequency value to 6.72 THz, the vibrations of Nb atoms are dominant. The average logarithmic frequency (ω_{ln} value calculated for the Nb_3Os compound, which is another parameter related to superconductivity, was found to be 222.97 K. The last parameter calculated for superconductivity is the superconducting transition temperature T_c. Allen-Dynes formula [42] was used to calculate this parameter. T_c value for Nb_3Os compound was calculated as 1.05 K. Our result is in good agreement with the previous experimental values of 1.02 K [4] and 0.943 K [5]. This harmony increases the reliability of the data obtained as a result of our study.

In order to better analyze the superconductivity properties of Nb_3Os compound, it will be useful to compare it with those of Nb_3Ge, which is the A15 material with the highest T_c temperature. According to BCS theory, $N(E_F)$ and λ parameters have an important role in determining the superconductivity properties of a material. If both of these parameters are large, it indicates that the superconducting transition temperature will also be large. In the experimental study conducted for Nb_3Ge in 1984, the $N(E_F)$ value was found to be approximately 12 States/eV, while λ was obtained as 1.4 [43]. In the theoretical study conducted using the FPLAPW method for Nb_3Ge, $N(E_F)$ and λ values were calculated as 14.4 States/eV and 1.8, respectively [44]. The experimental [43] and theoretical [44] $N(E_F)$ values obtained in previous studies for Nb_3Ge are more than twice the value of $N(E_F)$=5.31 states/eV obtained for Nb_3Os. In addition, the λ values obtained in the same studies [43,44] for Nb_3Ge are much larger than the result of λ=0.41 calculated in this study for Nb3Os. As a result of these comparisons, the $T_c = 1.05$ K value calculated for Nb_3Os is much smaller than the 23.2 K value obtained both theoretically [44] and experimentally [45] for Nb_3Ge.

4. Conclusion

In this study, structural, electronic, mechanical and superconductivity properties of Nb_3Os crystal have been investigated by using GGA and ab-initio plane wave methods based on DFT. The open-access QUANTUM ESPRESSO package programme was used in the calculations to investigate these properties. In the theoretical calculations, the generalised gradient approximation parametrised by Perdew-Burke-Ernzerhof was used to study exchange and correlation interactions. The structural parameters obtained as a result of geometrical optimisation for the Nb_3Os compound were found to be in very good agreement with the experimental and theoretical values presented previously in the literature. This result proves the accuracy of the theoretical

Table 3
Frequencies (THz) of optical phonon modes at the Γ point for Nb_3Os compound and calculated λ values for each.

Compound	$T_{1u}(I)$	$T_{2u}(S)$	$T_{1g}(S)$	$T_{1u}(I)$	$T_{2g}(R)$	$T_{2u}(S)$	$E_g(R)$	$A_{2g}(S)$
Nb_3Os (ν)	3.704	3.805	4.601	4.729	5.624	6.297	8.586	9.046
Nb_3Os (λ)	0.017	0.010	0.035	0.014	0.024	0.006	0.013	0.012

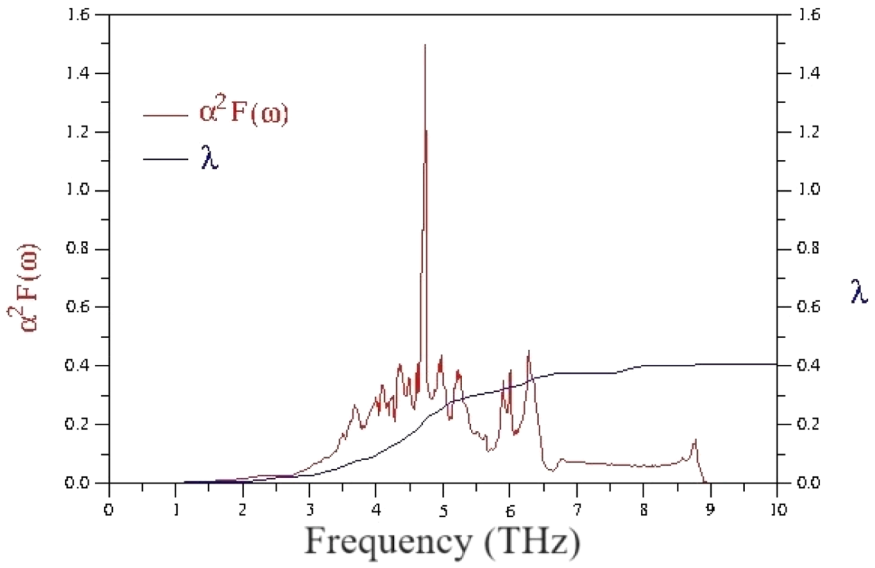

Fig. 6. Variation of electron-phonon interaction parameter and Eliashberg spectral function with frequency for Nb_3Os compound.

method we have chosen for the structural parameters and our calculations. After the determination of the structural parameters for the Nb_3Os compound, the electronic properties of this compound were also investigated using these parameters. When the electronic spectrum obtained was analysed, it was seen that it has a similar character with the previous theoretical results and confirms the metallic property of Nb_3Os compound. In addition, in the calculations for the electronic density of states, the $N(E_F)$ value, which has an important place in the determination of superconductivity properties, was obtained as 5.31 states/eV. When the partial electronic density of states was analysed, it was found that the largest contribution to the $N(E_F)$ value came from the 4d electrons of Nb atoms.

The main aim of this study is to theoretically investigate the origin of the superconductivity of Nb_3Os compound. For this purpose, the structural and electronic properties as well as the vibrational properties of Nb_3Os compound have been analysed in detail. As a result of these investigations, it was found that the Nb_3Os compound is dynamically stable and the phonon modes with low frequency contribute more to the electron-phonon interaction parameter. Finally, the superconductivity parameters of Nb_3Os compound obtained by using electronic and phonon properties together are presented. The electron-phonon interaction parameter (λ), logarithmic average phonon frequency (ω_{ln}) and superconductivity transition temperature (T_c) for Nb_3Os compound were determined as 0.41, 222.97 K and 1.05 K, respectively. The T_c value we calculated as 1.05 K for Nb_3Os compound is in very good agreement with the experimental value of 1.02 K. This result proves the reliability of our chosen method and calculations.

CRediT authorship contribution statement

Fatih Kurtuluş: Writing – review & editing, Writing – original draft, Methodology, Investigation, Conceptualization. **Ertuğrul Karaca:** Writing – review & editing, Writing – original draft, Methodology, Conceptualization. **Sadık Bağcı:** Writing – review & editing, Writing – original draft, Methodology, Conceptualization.

Declaration of competing interest

The authors declare that they have no known competing financial interests or personal relationships that could have appeared to influence the work reported in this paper

Data availability

No data was used for the research described in the article.

References

[1] G.F. Hardy, J.K. Hulm, Superconducting silicides and germanides, Phys. Rev 89 (1953) 884, https://doi.org/10.1103/PhysRev.89.884.
[2] J.G. Bednorz, K.A. Müller, Possible high Tc superconductivity in the Ba−La−Cu−O system, Zeitschrift für Physik B Condensed Matter 64 (1986) 189–193, https://doi.org/10.1007/BF01303701.
[3] L.R. Testardi, J.H. Wernick, W.A. Royer, Superconductivity with onset above 23°K in Nb-Ge sputtered films, Solid State Commun 15 (1974) 1–4, https://doi.org/10.1016/0038-1098(74)90002-7.
[4] B. Matthias, T. Geballe, V. Compton, Superconductivity, Rev. Mod. Phys 35 (1963) 1–22, https://doi.org/10.1103/revmodphys.35.1.
[5] R.D. Blaugher, R.E. Hein, J.E. Cox, R.M. Waterstrat, Atomic ordering and superconductivity in A-15 compounds, J. Low Temp. Phys 1 (1969) 539–561, https://doi.org/10.1007/BF00627932.
[6] D. Dew-Hughes, Superconducting A-15 compounds: a review, Cryogenics 15 (1975) 435–454, https://doi.org/10.1016/0011-2275(75)90019-3.
[7] M.S. Reddy, S.V. Suryanarayana, Lattice thermal expansion of Nb_3Os, J. Mater. Sci. Lett 2 (1983) 171–172, https://doi.org/10.1007/BF00735569.
[8] M.S. Reddy, S.V. Suryanarayana, Debye characteristic temperatures of Nb_3Os, Nb_3Pt and Nb_3Au, J. Mater. Sci. Lett 3 (1984) 763–766, https://doi.org/10.1007/BF00727967.
[9] H. Haas, Electric field gradients at V, Nb and Ta in A15 alloys, Hyperfine Interact 120 (1999) 157–161, https://doi.org/10.1023/A:1017094516580.
[10] C. Paduani, Electronic properties of the A-15 Nb-based intermetallics Nb_3(Os, Ir, Pt, Au), Solid State Commun 144 (2007) 352–356, https://doi.org/10.1016/j.ssc.2007.07.030.
[11] M.I. Naher, F. Parvin, A.K. Islam, S.H. Naqib, Physical properties of niobium-based intermetallics (Nb_3B; B= Os, Pt, Au): a DFT-based ab-initio study, Europ. Phys. J. B, 91 (2018) 1–13, https://doi.org/10.1140/epjb/e2018-90388-9.
[12] S. Bağcı, H.M. Tütüncü, S. Duman, G.P. Srivastava, Phonons and superconductivity in fcc and dhcp lanthanum, Phys. Rev. B 81 (2010) 144507, https://doi.org/10.1103/PhysRevB.81.144507.
[13] S. Baroni, S. De Gironcoli, A. Dal Corso, P. Giannozzi, Phonons and related crystal properties from density-functional perturbation theory, Rev. Mod. Phys 73 (2001) 515, https://doi.org/10.1103/RevModPhys.73.515.
[14] R. Bauer, A. Schmid, P. Pavone, D. Strauch, Electron-phonon coupling in the metallic elements Al, Au, Na, and Nb: a first-principles study, Phys. Rev. B 57 (1998) 11276, https://doi.org/10.1103/PhysRevB.57.11276.
[15] A.Y. Liu, A.A. Quong, Linear-response calculation of electron-phonon coupling parameters, Phys. Rev. B 53 (1996) R7575, https://doi.org/10.1103/PhysRevB.53.R7575.
[16] H.M. Tütüncü, S. Bağcı, G.P. Srivastava, Electronic structure, phonons, and electron-phonon interaction in Mo_3Si, Phys. Rev. B 82 (2010) 214510, https://doi.org/10.1103/PhysRevB.82.214510.
[17] H.M. Tütüncü, S. Bağcı, G.P. Srivastava, A. Akbulut, Electrons, phonons and superconductivity in rocksalt and tungsten–carbide phases of CrC, J. Phys 24 (2012) 455704, https://doi.org/10.1088/0953-8984/24/45/455704.

[18] F. Weber, S. Rosenkranz, L. Pintschovius, J.P. Castellan, R. Osborn, W. Reichardt, R. Heid, K.P. Bohnen, E.A. Goremychkin, A. Kreyssig, K. Hradil, D.L. Abernathy, Electron-phonon coupling in the conventional superconductor YNi2B2C at high phonon energies studied by time-of-flight neutron spectroscopy, Phys. Rev. Lett. 109 (2012) 057001, https://doi.org/10.1103/PhysRevLett.109.057001.
[19] P. Giannozzi, S. Baroni, N. Bonini, M. Calandra, R. Car, C. Cavazzoni, D. Ceresoli, G.L. Chiarotti, M. Cococcioni, I. Dabo, A. Dal Corso, S. De Gironcoli, S. Fabris, G. Fratesi, R. Gebauer, U. Gerstmann, C. Gougoussis, A. Kokalj, M. Lazzeri, L. Martin-Samos, N. Marzari, F. Mauri, R. Mazzarello, S. Paolini, A. Pasquarello, L. Paulatto, C. Sbraccia, S. Scandolo, G. Sclauzero, A.P. Seitsonen, A. Smogunov, P. Umari, R.M. Wentzcovitch, QUANTUM ESPRESSO: a modular and open-source software project for quantum simulations of materials, J. Phys 21 (2009) 395502, https://doi.org/10.1088/0953-8984/21/39/395502.
[20] J.P. Perdew, K. Burke, M. Ernzerhof, Generalized gradient approximation made simple, Phys. Rev. Lett. 77 (1996) 3865, https://doi.org/10.1103/PhysRevLett.77.3865.
[21] W. Kohn, L.J. Sham, Self-consistent equations including exchange and correlation effects, Phys. Rev 140 (1965) A1133, https://doi.org/10.1103/PhysRev.140.A1133.
[22] H.J. Monkhorst, J.D. Pack, Special points for Brillouin-zone integrations, Phys. Rev. B 13 (1976) 5188, https://doi.org/10.1103/PhysRevB.13.5188.
[23] A.B. Migdal, Interaction between electrons and lattice vibrations in a normal metal, Sov. Phys. JETP 7 (1958) 996–1001.
[24] G.M. Eliashberg, Interactions between electrons and lattice vibrations in a superconductor, Sov. Phys. JETP 11 (1960) 696–702.
[25] W.L. McMillan, Transition temperature of strong-coupled superconductors, Phys. Rev. 167 (1968) 331.
[26] J.P. Carbotte, Properties of boson-exchange superconductors, Rev. Mod. Phys. 62 (1990) 1027.
[27] B. Cordero, V. Gómez, A.E. Platero-Prats, M. Revés, J. Echeverría, E. Cremades, F. Barragán, S. Alvarez, Covalent radii revisited, Dalton Transac 21 (2008) 2832–2838, https://doi.org/10.1039/B801115J.
[28] P. Pyykkö, M. Atsumi, Molecular double-bond covalent radii for elements Li–E112, Chemistry, 15 (2009) 12770–12779, https://doi.org/10.1002/chem.200901472.
[29] E. Karaca, P.J.P. Byrne, P.J. Hasnip, H.M. Tütüncü, M.I.J. Probert, Electron–phonon interaction and superconductivity in hexagonal ternary carbides Nb_2AC (A: al, S, Ge, As and Sn), Electr. Struc 3 (2021) 045001, https://doi.org/10.1088/2516-1075/ac2c94.
[30] F.D. Murnaghan, The compressibility of media under extreme pressures, Proceed. National Acad. Sci 30 (1944) 244–247, https://doi.org/10.1073/pnas.30.9.244.
[31] P.A. Beck (Ed.), Electronic Structure and Alloy Chemistry of the Transition Elements, Institute of Metals Division, The Metallurgical Society, American Institute of Mining, Metallurgical, and Petroleum Engineers. Interscience Publishers, 1963. Based on a symposium held in New York, February 22, 1962, and sponsored by the.
[32] Nevit, M.V. Intermetallics Compounds, edited by JH Westbrook. RE Krieger (Publishing Co, Huntington, NY), 1977.
[33] A. Dal Corso, Elastic constants of beryllium: a first-principles investigation, J. Phys 28 (2016) 075401, https://doi.org/10.1088/0953-8984/28/7/075401.
[34] A. Afaq, M. Rizwan, A. Bakar, Computational investigations of XMgGa (X= Li, Na) half Heusler compounds for thermo-elastic and vibrational properties, Phys. B 554 (2019) 102–106, https://doi.org/10.1016/j.physb.2018.11.013.
[35] D. Heciri, H. Belkhir, R. Belghit, B. Bouhafs, R. Khenata, R. Ahmed, A. Bouhemadou, T. Ouahrani, X. Wang, S.B. Omran, Insight into the structural, elastic and electronic properties of tetragonal inter-alkali metal chalcogenides CsNaX (X= S, Se, and Te) from first-principles calculations, Mater. Chem. Phys 221 (2019) 125–137, https://doi.org/10.1016/j.matchemphys.2018.09.024.
[36] Y. Han, Y. Wu, T. Li, R. Khenata, T. Yang, X. Wang, Electronic, magnetic, half-metallic, and mechanical properties of a new equiatomic quaternary Heusler compound YRhTiGe: a first-principles study, Materials 11 (2018) 797, https://doi.org/10.3390/ma11050797.
[37] D. Chen, Z. Chen, Y. Wu, M. Wang, N. Ma, H. Wang, First-principles investigation of mechanical, electronic and optical properties of Al_3Sc intermetallic compound under pressure, Comput. Mater. Sci 91 (2014) 165–172, https://doi.org/10.1016/j.commatsci.2014.05.007.
[38] M.U. Salma, M.A. Rahman, Study of structural, elastic, electronic, mechanical, optical and thermodynamic properties of $NdPb_3$ intermetallic compound: DFT based calculations, Comput. Conden. Matter 15 (2018) 42–47, https://doi.org/10.1016/j.cocom.2018.04.001.
[39] X. Luan, H. Qin, F. Liu, Z. Dai, Y. Yi, Q. Li, The mechanical properties and elastic anisotropies of cubic Ni_3Al from first principles calculations, Crystals 8 (2018) 307, https://doi.org/10.3390/cryst8080307.
[40] F. Sultana, M.M. Uddin, M.A. Ali, M.M. Hossain, S.H. Naqib, A.K.M.A. Islam, First principles study of M_2InC (M= Zr, Hf and Ta) MAX phases: the effect of M atomic species, Result. Phys 11 (2018) 869–876, https://doi.org/10.1016/j.rinp.2018.10.044.
[41] N. Lebga, S. Daoud, X.W. Sun, N. Bioud, A. Latreche, Mechanical and thermophysical properties of cubic rock-salt AlN under high pressure, J. Electr. Mater 47 (2018) 3430–3439, https://doi.org/10.1007/s11664-018-6169-x.
[42] P.B. Allen, R.C. Dynes, Transition temperature of strong-coupled superconductors reanalyzed, Phys. Rev. B 12 (1975) 905, https://doi.org/10.1103/PhysRevB.12.905.
[43] K.E. Kihlstrom, D. Mael, T.H. Geballe, Tunneling $\alpha^2F(\omega)$ and heat-capacitymeasurements in high-T_c Nb_3Ge, Phys. Rev. B 29 (1984) 150, https://doi.org/10.1103/PhysRevB.29.150.
[44] C. Paduani, Electronic structure and Fermi surfaces of the superconductive A_3B compounds: a = V, Nb; B = Ga, Ge and Sn, Solid State Commun 149 (2009) 1269, https://doi.org/10.1016/j.ssc.2009.05.011.
[45] L.R. Testardi, J.H. Wernick, W.A. Royer, Superconductivity with onset above 23K in Nb3Ge sputtered films, Solid State Commun 15 (1974) 1, https://doi.org/10.1016/0038-1098(74)90002-7.